Aerosol Science and Technology
Publication details, including instructions for authors and subscription information:
http://www.tandfonline.com/loi/uast20

A Numerical Study of the Effects of a Moving Operator on Particles in a Cleanroom with a Curtain

Wu-Shung Fu [a], Shih-Fa Chen [a] & Suh-Jenq Yang [a]
[a] Department of Mechanical Engineering, National Chiao Tung University, Hsinchu, Taiwan, Republic of China
Published online: 30 Nov 2010.

Aerosol Science and Technology 36: 154–161 (2002)

Published by Taylor and Francis
0278-6826/02/$12.00 + .00

A Numerical Study of the Effects of a Moving Operator on Particles in a Cleanroom with a Curtain

Wu-Shung Fu, Shih-Fa Chen, and Suh-Jenq Yang
Department of Mechanical Engineering, National Chiao Tung University, Hsinchu, Taiwan, Republic of China

The motion of airflow and particles induced by a moving operator in a cleanroom installed with a solid worktable and a vertical isolating curtain were studied numerically. This situation is classified as a kind of moving boundary problem, and a Galerkin finite element formulation with an arbitrary Lagrangian–Eulerian kinematic description method is adopted to analyze this problem. Two different moving speeds of the operator under Reynolds number Re = 500 and Schmidt number Sc = 1.0 are taken into consideration. The results show that recirculation zones, which are disadvantageous to remove the particles, are observed around the operator and near the worktable. The behavior of the operator usually prevents the particles from being removed, and the higher moving speed of the operator demonstrates that the removal of particles becomes more difficult. These phenomena are quite different from those that regard the moving operator as stationary in the cleanroom.

INTRODUCTION

For guaranteeing quality and stability of a precision device, a fabrication workshop must be a contamination controlled environment. This environment is usually called a cleanroom. To keep cleanliness in the cleanroom, the airflow supplied from the external environment entering the cleanroom must be filtered by a HEPA filter bank. Then the external airflow in the cleanroom becomes particle-free and plays a role in removing particles and hazardous gas that are usually generated by operators and equipment in the cleanroom.

In order to remove the particles in the cleanroom efficiently, several studies investigated the motion of particles in the airflow. Ermak and Buckholz (1980) simulated the effect of the airflow on the characteristics of the particles by using a Monte Carlo method, and the results showed that the characteristics of the particles were dominated by the airflow. Kuehn (1988), Yamamoto et al. (1988a,b), Yamamoto (1990), Busnaina et al. (1988), Kuehn et al. (1988), and Lemaire and Luscuere (1991) adopted the computational methods to investigate the airflow patterns and contaminant diffusion in the cleanroom. Settles and Via (1988) utilized Schlieren observations to observe the flow paths of the particles in the cleanroom. In addition, Liu and Ahn (1987) used the analogy between the mass and heat transfers to determine the particles deposition rates by diffusion. Donovan (1990) reviewed and summarized the development of the particle control for semiconductor manufacturing.

Based upon the above literature, the operator is doubtless a kind of serious contaminant source and the removal of particles generated by the operator becomes an important issue. To facilitate the analysis, most studies mentioned above regarded the moving operator as a stationary object when they investigated the effects of the airflow induced by the moving operator in the cleanroom on the particle diffusion. However, the motion of the operator regarded as stationary is quite different from that regarded as a moving object.

Furthermore, in a high quality cleanroom the behavior of particles has gradually become focused on particles that are smaller than 0.1 μm, so the diffusion effect becomes the main mechanism for the movement of the above particle. Therefore the motion of a small particle in the cleanroom is reasonably and conveniently assumed to be a mass transfer model of gas.

Consequently, the aim of this paper is to investigate numerically the effects of the movement of the operator and the vertical isolating curtain on the motions of the air and particles. An appropriate kinematic description method of the arbitrary Lagrangian–Eulerian (ALE) method (Noh 1964) is adopted to analyze the above phenomena. A Galerkin finite element method with moving mesh and a backward difference scheme dealing with the time terms are used to solve the governing equations. The results show that the airflow and particle transports in the cleanroom are deeply influenced by the movement of the operator. These phenomena are quite different from those of the moving operator regarded as a stationary one. From the viewpoint

Received 13 March 2000; accepted 13 April 2001.
The support of this work by the National Science Council of Taiwan, R.O.C., under contract NSC89-2212-E-009-019 is gratefully acknowledged.
Address correspondence to Professor Wu-Shung Fu, Department of Mechanical Engineering, National Chiao Tung University, 1001 Ta Hsueh Road, Hsinchu, 30056, Taiwan, Republic of China. E-mail: wsfu@cc.nctu.edu.tw

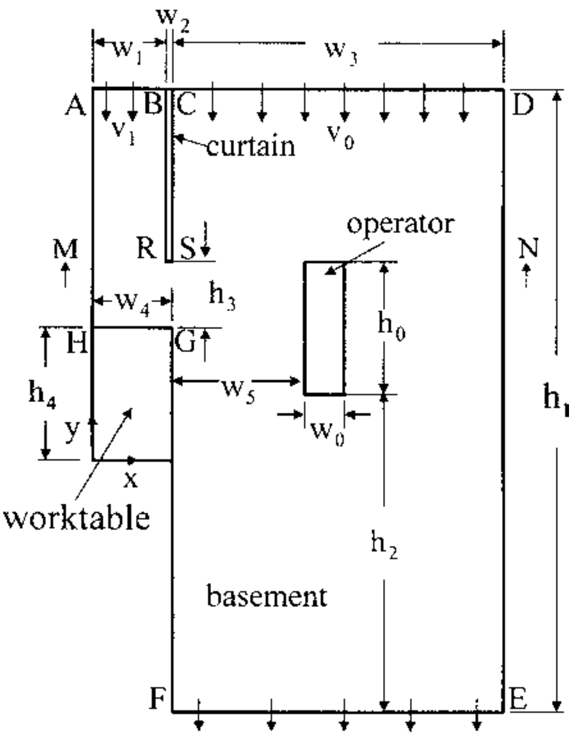

Figure 1. Physical model.

of removing particles, the relatively smaller moving velocity of the operator or the relatively larger velocity of the inlet airflow is expected.

PHYSICAL MODEL

The two-dimensional model of a vertical laminar flow cleanroom with a vertical isolating curtain and an operator sketched in Figure 1 is used. The width and height of the cleanroom are $w(= w_1 + w_2 + w_3)$ and h_1, respectively. A rectangular block with height h_0 and width w_0 is used to simulate an operator. The distance from the outlet of the cleanroom to the bottom surface of the operator is h_2. A worktable with height h_4 and width $w_4(= w_1 + w_2)$ is set on the left side, and the distance from the worktable to the operator is w_5. A vertical isolating curtain with width w_2 divides the inlet of the airflows into two sections of $\overline{AB}$ and $\overline{CD}$, respectively. The distance from the worktable to the curtain is h_3, and the curtain extends downward to the same level as the operator. Two different air inlet velocities are v_1 and v_0 flowing at the inlet sections of $\overline{AB}$ and $\overline{CD}$, respectively. Initially ($t = 0$), the operator is stationary and the airflow flows steadily. As the time $t > 0$, the operator moves to the worktable with a constant velocity u_b and stays beside the worktable, then finally leaves the worktable. Therefore the motion of the particles are affected by both the airflow and the movement of the operator, and the problem is described by a transient state. Thus the ALE method is properly utilized to analyze this problem.

In order to facilitate the analysis, the following assumptions are made.

1. The fluid is air and the flow field is two-dimensional, incompressible, and laminar.
2. The fluid properties are constant and the effect of gravity is neglected.
3. The no-slip condition is held on the interfaces between the airflow and operator.
4. The concentration of particles on the operator surface is constant and equal to c_0.

According to the characteristic scales of w_0, v_0, ρv_0^2, and c_0, the dimensionless variables are defined as follows:

$$X = \frac{x}{w_0}, \quad Y = \frac{y}{w_0}, \quad U = \frac{u}{v_0}, \quad V = \frac{v}{v_0},$$
$$\hat{U} = \frac{\hat{u}}{v_0}, \quad U_b = \frac{u_b}{v_0}, \quad P = \frac{p - p_\infty}{\rho v_0^2}, \quad \tau = \frac{t v_0}{w_0}, \quad [1]$$
$$C = \frac{c}{c_0}, \quad \mathrm{Re} = \frac{v_0 w_0}{\nu}, \quad \mathrm{Sc} = \frac{\nu}{D},$$

where $\hat{u}$ is the mesh velocity.

Based on the above assumptions and dimensionless variables, the dimensionless ALE governing equations are expressed as the following equations:

continuity equation:

$$\frac{\partial U}{\partial X} + \frac{\partial V}{\partial Y} = 0; \quad [2]$$

momentum equations:

$$\frac{\partial U}{\partial \tau} + (U - \hat{U})\frac{\partial U}{\partial X} + V\frac{\partial U}{\partial Y} = -\frac{\partial P}{\partial X} + \frac{1}{\mathrm{Re}}\left(\frac{\partial^2 U}{\partial X^2} + \frac{\partial^2 U}{\partial Y^2}\right); \quad [3]$$

$$\frac{\partial V}{\partial \tau} + (U - \hat{U})\frac{\partial V}{\partial X} + V\frac{\partial V}{\partial Y} = -\frac{\partial P}{\partial Y} + \frac{1}{\mathrm{Re}}\left(\frac{\partial^2 V}{\partial X^2} + \frac{\partial^2 V}{\partial Y^2}\right); \quad [4]$$

concentration diffusion equation:

$$\frac{\partial C}{\partial \tau} + (U - \hat{U})\frac{\partial C}{\partial X} + V\frac{\partial C}{\partial Y} = \frac{1}{\mathrm{Re\,Sc}}\left(\frac{\partial^2 C}{\partial X^2} + \frac{\partial^2 C}{\partial Y^2}\right). \quad [5]$$

As the time $\tau > 0$, the boundary conditions are as follows: on the wall surfaces of $\overline{DE}$, $\overline{FG}$, and $\overline{AH}$:

$$U = V = 0, \quad \frac{\partial C}{\partial X} = 0; \quad [6]$$

on the wall surface of $\overline{GH}$:

$$U = V = 0, \quad \frac{\partial C}{\partial Y} = 0; \quad [7]$$

on the curtain surfaces of $\overline{BR}$ and $\overline{CS}$:

$$U = V = 0, \quad \frac{\partial C}{\partial X} = 0; \quad [8]$$

on the curtain surface of $\overline{RS}$:

$$U = V = 0, \qquad \frac{\partial C}{\partial Y} = 0; \qquad [9]$$

on the airflow inlet section of $\overline{AB}$:

$$U = C = 0, \qquad V = -1.25; \qquad [10]$$

on the airflow inlet section of $\overline{CD}$:

$$U = C = 0, \qquad V = -1.0; \qquad [11]$$

on the airflow outlet section of $\overline{EF}$:

$$\frac{\partial U}{\partial Y} = \frac{\partial V}{\partial Y} = \frac{\partial C}{\partial Y} = 0; \qquad [12]$$

on the interfaces of the operator and the airflow:

$$U = U_b, \qquad V = 0, \qquad C = 1. \qquad [13]$$

NUMERICAL METHOD

A Galerkin finite element formulation with moving meshes and an implicit scheme dealing with the time terms are adopted to solve the governing equations (Equations (2)–(5)). Newton–Raphson iteration algorithm and a penalty function model (Reddy and Gartling 1994) are utilized to handle the nonlinear and pressure terms in the momentum equations, respectively. The velocity and concentration terms are expressed as quadrilateral and nine-node quadratic isoparametric elements. The discretization processes of the governing equations are similar to the one used in Fu et al. (1990). Then the momentum equations (Equations (3)–(4)) can be expressed as follows:

$$\sum_{1}^{n_e} \left([A]^{(e)} + [K]^{(e)} + \lambda[L]^{(e)}\right)\{q\}^{(e)}_{\tau+\Delta\tau} = \sum_{1}^{n_e}\{f\}^{(e)}, \qquad [14]$$

where

$$\left(\{q\}^{(e)}_{\tau+\Delta\tau}\right)^T = \langle U_1, U_2, \ldots, U_9, V_1, V_2, \ldots, V_9\rangle^{m+1}_{\tau+\Delta\tau}, \qquad [15]$$

$[A]^{(e)}$ consists of the mth iteration values of U and V at the time $\tau + \Delta\tau$, $[K]^{(e)}$ consists of the shape function, $\hat{U}$, and time differential terms, $[L]^{(e)}$ consists of the penalty function terms, $\{f\}^{(e)}$ consists of the known values of U and V at the time τ and mth iteration values of U and V at the time $\tau + \Delta\tau$.
The concentration Equation (5) can be expressed as follows:

$$\sum_{1}^{n_e} \left([M]^{(e)} + [Z]^{(e)}\right)\{c\}^{(e)}_{\tau+\Delta\tau} = \sum_{1}^{n_e}\{r\}^{(e)}, \qquad [16]$$

where

$$\left(\{c\}^{(e)}_{\tau+\Delta\tau}\right)^T = \langle C_1, C_2, \ldots C_9\rangle_{\tau+\Delta\tau}, \qquad [17]$$

$[M]^{(e)}$ consists of the values of U and V at time $\tau + \Delta\tau$, $[Z]^{(e)}$ consists of the shape function, $\hat{V}$, and time differential terms, $\{r\}^{(e)}$ consists of the known values of C at time τ.

In Equations (14) and (16), the terms with the penalty parameter λ are integrated by 2×2 Gaussian quadrature, and the other terms are integrated by 3×3 Gaussian quadrature. The value of the penalty parameter used in this study is 10^6 and the frontal method solver is applied to solve Equations (14) and (16). The mesh velocity $\hat{U}$ is assumed to be linearly distributed and inversely proportional to the distance between the node and operator.

A brief outline of the solution procedure is described as follows:

1. Determine the optimal mesh distribution and number of the elements and nodes.
2. Solve the values of U and V at the steady state and regard them as the initial values.
3. Determine the time increment $\Delta\tau$ and the mesh velocities $\hat{U}$ at every node.
4. Update the coordinates of the nodes and examine the determinant of the Jacobian transformation matrix to ensure the one-to-one mapping to be satisfied during the Gaussian quadrature numerical integration, otherwise execute the mesh reconstruction.
5. Solve Equation (14) until the following criteria for convergence are satisfied:

$$\left|\frac{\phi^{m+1} - \phi^m}{\phi^{m+1}}\right|_{\tau+\Delta\tau} < 10^{-3}, \text{ where } \phi = U, V. \qquad [18]$$

6. Substitute U and V into Equation (16) to obtain C.
7. Continue the next time step calculation until the assigned position of the operator is reached.

RESULTS AND DISCUSSION

For analyzing conveniently, the dimensionless parameters are adopted. The dimensionless length $H_2(= h_2/w_0)$ is determined by numerical tests and is equal to 18.0 to satisfy the boundary condition at the outlet of the airflow. At the time $\tau = 0.0$, the distance from the worktable to the operator is $W_5 = 4.5$.

Concerning the diffusion coefficient D of the particles, the diffusion coefficient decreases as the diameter of the particle increases (Hinds 1982) and the Schmidt number, Sc, is in inverse ratio to the diameter of the particles. For facilitating the analysis, the value of Sc is assumed to be 1.0, which is an appropriate value for most gases and is the worst limiting situation for the diffusion of the particle.

Two different moving speeds, 2.0 and 0.75, of the operator are taken into consideration under Re = 500 and Sc = 1.0 situations for examining the effects of the moving speed on the flow field, which dominates the removing of particles. In order to obtain the optimal computational meshes and time step, a series of numerical tests are executed. Three different nonuniform distribution elements, 3612, 4048, and 4804 (corresponding to

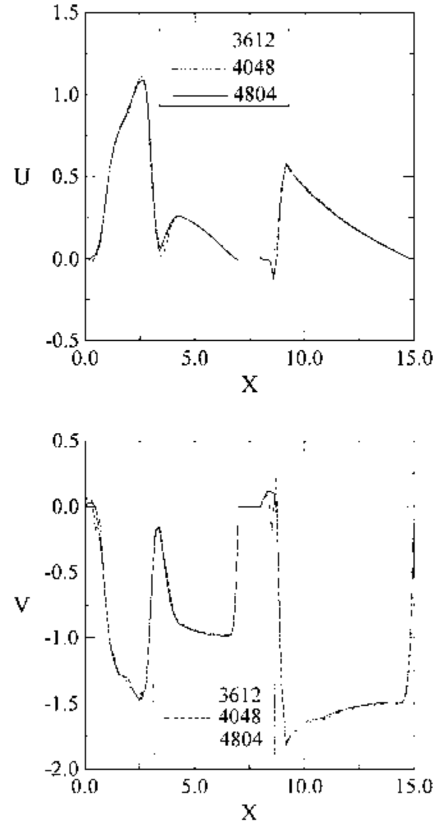

Figure 2. Comparison of the distribution of the velocities U and V along the line $\overline{MN}$ at the steady state and Re = 500 for various meshes.

14816, 16572, and 19640 nodes, respectively), are used for the mesh tests at the steady state and Re = 500 situation. The results of the velocities U and V distributions along the line $\overline{MN}$ as shown in Figure 1 are indicated in Figure 2. According to the results of the mesh tests, the computational mesh with 4804 elements is adopted. As for the selection of the time step $\Delta\tau$, three different time steps, 0.05, 0.01, and 0.005, at Re = 500 and the moving velocity of the operator $U_b = -2.0$ are executed. Similarly, the distributions of the velocities U and V along the line $\overline{MN}$ at the time $\tau = 2.0$ are shown in Figure 3. The variations of the velocities U and V of the above different time steps are consistent, and the time step $\Delta\tau = 0.01$ is chosen.

The dimensionless stream function Ψ is defined as

$$U = \frac{\partial \Psi}{\partial Y} \quad \text{and} \quad V = -\frac{\partial \Psi}{\partial X}. \qquad [19]$$

For illustrating the flow and concentration fields more clearly, the phenomena around the work region are presented only.

Figure 4 shows the transient developments of the streamlines of the flow field and constant concentration lines of the particle diffusion around the work area for the moving speed of the operator being equal to 2.0 case. At time $\tau = 0.0$, as shown in Figure 4(a), the operator is stationary and the airflow flows steadily. Several recirculation zones are found near the top and

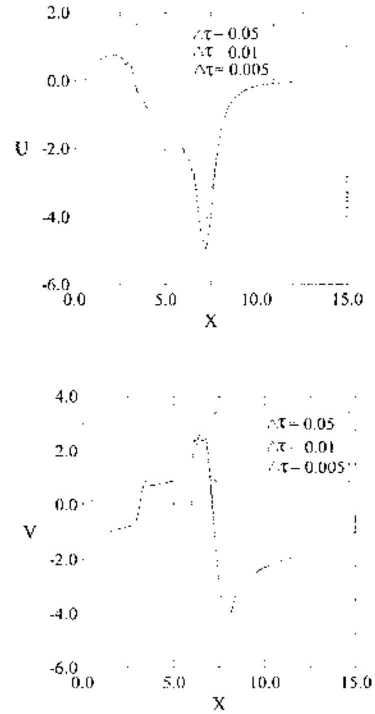

Figure 3. Comparison of the distribution of the velocities U and V along the line $\overline{MN}$ for various time steps under the moving velocity of the arm $U_b = -2.0$ and Re = 500 at the time $\tau = 2.0$

lateral surfaces of the worktable. These recirculation zones are not favorable to remove the particles. At time $\tau > 0.0$, the operator starts to move toward the worktable with a constant moving velocity of $U_b = -2.0$ and the variations of the flow and concentration fields become the transient state. At time $\tau = 0.2$ (Figure 4b), the space between the worktable and operator is contracted, which results in the airflow beginning to flow to the rear region of the operator. The airflow from the inlet section $\overline{CD}$ is remarkably affected by the movement of the operator. As the time increases, as shown in Figures 4c–d, the space between the worktable and operator becomes narrow, then most inlet airflows from sections $\overline{AB}$ and $\overline{CD}$ flow around the rear region of the operator. In this duration, the new airflow induced by the moving operator is forced to flow over the worktable and sweeps away the original recirculation zones forming on the worktable. Afterward, the new airflow joins with the airflow from the inlet and flow together to the rear region of the operator. In the meantime, the recirculation zones in the rear region of the operator and on the outside of the bottom of the curtain enlarge gradually, which is disadvantageous to the removal of particles.

As for the distributions of the constant concentration lines, most particles are removed by the airflow, and the residual particles usually suspend within the recirculation zones. Shown in Figures 4c–d, the space between the worktable and operator becomes narrow as the operator moves to the worktable. Consequently, the effect of the airflow from the inlet on the

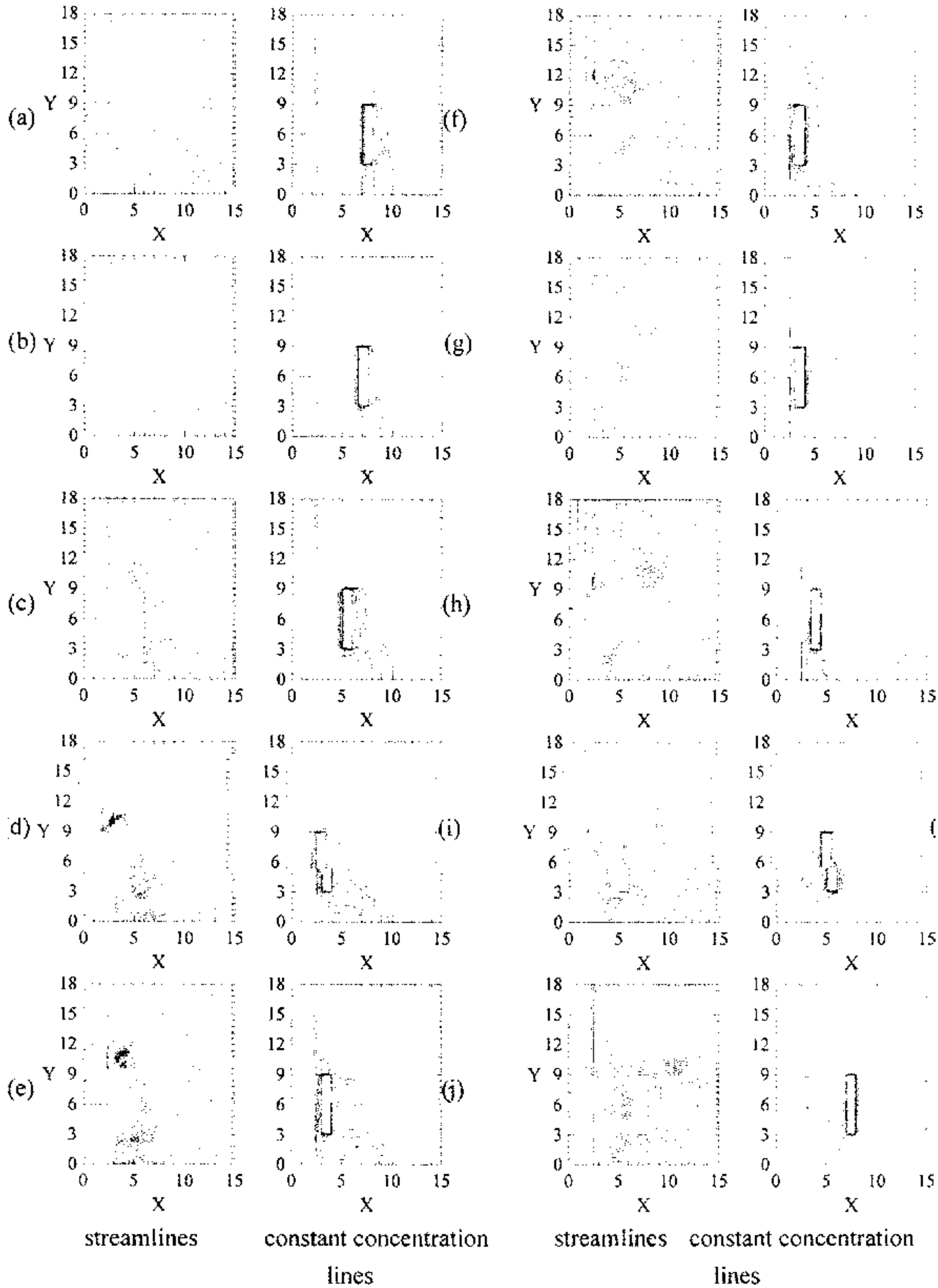

Figure 4. Transient developments of the streamlines and constant concentration lines distributions around the work area of the cleanroom for the operator moving speed equal to 2.0 case (a) $\tau = 0.0$, $U_b = 0.0$; (b) $\tau = 0.2$, $U_b = -2.0$; (c) $\tau = 1.0$, $U_b = -2.0$; (d) $\tau = 2.0$, $U_b = -2.0$; (e) $\tau = 2.2$, $U_b = 0.0$; (f) $\tau = 4.5$, $U_b = 0.0$; (g) $\tau = 7.0$, $U_b = 0.0$; (h) $\tau = 7.0$, $U_b = 2.0$; (i) $\tau = 8.0$, $U_b = 2.0$; (j) $\tau = 9.0$, $U_b = 2.0$.

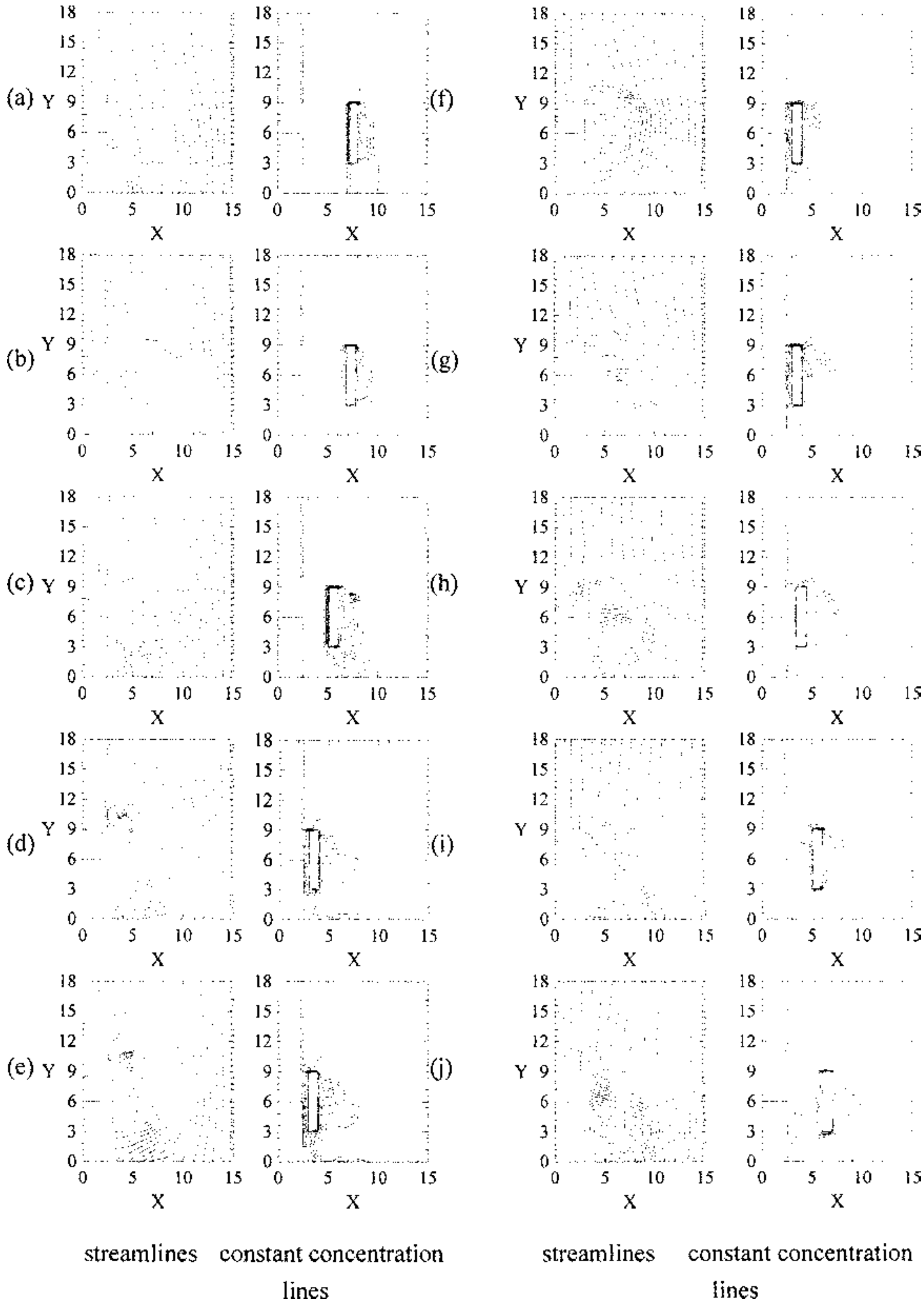

Figure 5. Transient developments of the streamlines and constant concentration lines distributions around the work area of the cleanroom for the operator moving speed equal to 0.75 case (a) $\tau = 0.0$, $U_b = 0.0$; (b) $\tau = 0.26$, $U_b = -0.75$; (c) $\tau = 2.6$, $U_b = -0.75$; (d) $\tau = 5.33$, $U_b = -0.75$; (e) $\tau = 5.6$, $U_b = 0.0$; (f) $\tau = 7.83$, $U_b = 0.0$; (g) $\tau = 10.33$, $U_b = 0.0$; (h) $\tau = 10.6$, $U_b = 0.75$; (i) $\tau = 13.0$, $U_b = 0.75$; (j) $\tau = 14.33$, $U_b = 0.75$.

removing of the particles is reduced, then the particles suspending in this space diffuse to the worktable gradually.

During the time τ from 2.0 to 7.0, the operator stays beside the worktable ($U_b = 0.0$), as shown in Figures 4e–g. The recirculation zones on the outside of the curtain are swept away gradually. However, a new recirculation zone forms on the worktable, and most airflows from the inlet section $\overline{AB}$ flow around the bottom surface of the curtain and to the outside, which hardly destroys the new recirculation zone. As a result, the particles easily suspend in this recirculation zone; this could damage the product on the worktable.

At time $\tau > 7.0$ (Figures 4h–j), the operator leaves the worktable with a constant velocity $U_b = 2.0$. Since the operator moves to the right, the airflow from the inlet is affected by the operator and also flows to the right. The space mentioned above becomes broad gradually, and the inlet airflow easily passes through this space, which causes the recirculation zones near the worktable and operator to be decreased gradually, but new recirculation zones appear in the low region beside the worktable.

Concerning the distributions of the constant concentration lines, accompanying the variations of the airflow mentioned above, the particles distributed around the worktable are swept by the airflow from the inlet gradually. As the time increases, most particles distribute around the operator and are far away the worktable.

Figure 5 shows the transient development of the distributions of the streamlines and constant concentration lines for the moving speed of the operator being equal to 0.75. At time $\tau > 0$, the operator starts to move toward the worktable with a constant velocity of $U_b = -0.75$. If the moving speed of the operator is smaller than the airflow inlet velocity, then the airflow flows easily through the space between the worktable and operator (Figure 5c) until the operator is very close to the worktable (Figure 5d). These phenomena shown in Figure 5 are different from those shown in Figure 4. Besides, the airflow induced by the operator is not so significant due to the smaller moving speed of the operator, and the variations of the flow fields are relatively simple. The recirculation zones are still observed around the operator, but the strength of the recirculation zones is smaller than that of the above case. Consequently, the particles suspending in these recirculation zones are possibly removed by the airflow. For the same reason, the constant concentration lines of particles cannot diffuse so broadly as those of the above case (Figure 4).

During the time τ from 5.33 to 10.33, the operator stays beside the worktable ($U_b = 0.0$). As shown in Figures 5e–g, the recirculation zones around the operator are shrunk gradually with increasing time, and most particles can be swept away by the airflow in the cleanroom.

At time $\tau > 10.33$, the operator leaves the worktable with a constant moving velocity of $U_b = 0.75$. In Figures 5h–j, the recirculation zones newly form around the bottom surface of the operator and the lateral surface of the worktable due to the movement of the operator. Since the airflow from the inlet dominates the flow field, the variations of the airflow are simple and beneficial to the removal of the particles.

CONCLUSIONS

The motion of the air and particles induced by the movement of an operator in a cleanroom with a solid worktable and a vertical isolating curtain are investigated numerically. The results can be summarized as follows:

1. The airflow and particle transport in the cleanroom are deeply influenced by the movement of the operator. These phenomena are quite different from those of the moving operator regarded as a stationary one.
2. The effects of the moving speed of the operator on the motion of the airflow and particles are remarkable. From the viewpoint of removing particles, the relatively smaller moving velocity of the operator or the relatively larger velocity of the inlet airflow is expected.

NOMENCLATURE

c_0	dimensional concentration of particle on the operator [Kg/m^3]
C	dimensionless concentration of particle ($C = c/c_0$)
D	diffusion coefficient of the concentration of the particle [m^2/s]
H_0	dimensionless height of the operator
H_1	dimensionless height of the cleanroom
H_2	dimensionless distance from the outlet of the cleanroom to the operator
H_3	dimensionless distance from the worktable to the curtain
H_4	dimensionless height of the worktable
p	dimensional pressure [N/m^2]
p_∞	reference pressure [N/m^2]
P	dimensionless pressure ($P = (p - p_\infty)/\rho v_0^2$)
Re	Reynolds number (Re $= v_0 w_0/\nu$)
Sc	Schmidt number (Sc $= \nu/D$)
t	dimensional time [s]
u_b	dimensional moving velocity of the operator [m/s]
$\hat{u}$	dimensionless mesh velocity in x-direction [m/s]
$\hat{U}$	dimensionless mesh velocity in X-direction
U_b	dimensionless moving velocity of the operator
U, V	dimensionless velocities of the airflow in X and Y directions
v_0	dimensional airflow inlet velocity at a section of $\overline{CD}$ [m/s]
V_0	dimensionless airflow inlet velocity at a section of $\overline{CD}$
V_1	dimensionless airflow inlet velocity at a section of $\overline{AB}$
w_0	dimensional width of the operator [m]
W	dimensionless width of the cleanroom
W_0	dimensionless width of the operator
W_1	dimensionless width of the airflow inlet section $\overline{AB}$
W_2	dimensionless width of the curtain

W_3 dimensionless width of the airflow inlet section $\overline{CD}$
W_4 dimensionless width of the worktable
W_5 dimensionless distance from the worktable to the operator
x, y dimensional Cartesian coordinates [m]
X, Y dimensionless Cartesian coordinates

Greek Symbols

λ penalty parameter
ν kinematic viscosity [m^2/s]
ρ density [Kg/m^3]
τ dimensionless time ($\tau = tv_0/w_0$)
Ψ dimensionless stream function

Superscripts

(e) element
m iteration number
T transpose matrix

Other

[ ] matrix
{ } column vector
⟨ ⟩ row vector

REFERENCES

Busnaina, A. A., Abuzeid, S., and Sharif, M. A. R. (1988). *Numerical Modeling of Fluid Flow and Particle Transport in Clean Room*, Proceedings of the 9th International Committee Contamination Control Societies Conference, Los Angeles, pp. 600–607.

Donovan, R. P. (1990). *Particle Control for Semiconductor Manufacturing*, Marcel Dekker Inc., New York.

Ermak, D. L., and Buckholz, H. (1980). Numerical Integration of the Langerin Equation: Monte Carlo Simulation, *J. Comput. Phys*. 35:169–182.

Fu, W. S., Kau, T. M., and Shieh, W. J. (1990). Transient Laminar Natural Convection in an Enclosure from Steady Flow State to Stationary State, *Numer. Heat Trans. A* 18:189–211.

Hinds, W. C. (1982). *Aerosol Technology*, John Wiley & Sons, New York.

Kuehn, T. H. (1988). Computer Simulation of Airflow and Particle Transport in Cleanrooms, *J. Environ. Sci.* 31(5):21–27.

Kuehn, T. H., Marple, V. A., Han, H., Liu, D., Shanmugavelu, I., and Youssef, S. W. (1988). Comparison of Measured and Predicted Airflow Patterns in a Clean Room, *Proceedings-Institute of Environmental Science* 98(2):331–336.

Lemaire, T., and Luscuere, P. (1991). Investigating Computer Modeling of Cleanroom Airflow Patterns, *Microcontamination* 9(8):19–26.

Liu, B. Y. H., and Anh, K. (1987). Particle Deposition on Semiconductor Wafers, *Aerosol Sci. Technol.* 6(3):215–224.

Noh, W. F. (1964). *A Time-Dependent Two-Space-Dimensional Coupled Eulerian-Lagrangian Code, Methods in Computational Physics*, Vol. 3, edited by B. Alder, S. Fernbach and M. Rotenberg. Academic Press, New York, p. 117.

Settles, G. S., and Via, G. G. (1988). A Portable Schlieren System for Clean-Room Airflow Analysis, *J. Environ. Sci.* 30(5):17–21.

Yamamoto, T. (1990). *Airflow Modeling and Particle Control by Vertical Laminar Flow, Particle Control for Semiconductor Manufacturing*, edited by R. P. Donovan. Marcel Dekker Inc., New York, pp. 301–323.

Yamamoto, T., Donovan, R. P., and Ensor, D. S. (1988a). Numerical Simulation of Clean Room Air Flows, *Int. J. of Engineering Fluid Mechanics* 1:134–150.

Yamamoto, T., Donovan, R. P., and Ensor, D. S. (1988b). Model Study for Optimization of Cleanroom Airflow, *J. Environ. Sci.* 31(6):24–29.